

Lightning occurrences and intensity over the Indian region: Long-term trends and future projections

Rohit Chakraborty¹, Arindam Chakraborty^{2,3}, Ghouse Basha⁴ and Madineni Venkat Ratnam⁴

¹ Divecha Centre for Climate Change, Indian Institute of Science, India

² Centre for Atmospheric and Oceanic Studies, Indian Institute of Science, India

³ DST-Centre of Excellence in Climate Change, Divecha Centre for Climate Change, IISc, India

⁴ National Atmospheric Research Laboratory, India

Correspondence to: Rohit Chakraborty (rohitchakrab@iisc.ac.in)

Abstract

Lightning activities constitute the major destructive component of thunderstorms over India. Hence, understanding the long-term variabilities of lightning occurrence and intensity and their inter-relation with various causative factors is required. Long-term (1998-2014) Tropical Rainfall Measuring Mission (TRMM) satellite-based lightning observations depict the most frequent lightning occurrences along the Himalayan foothills, the Indo-Gangetic plains and coastal regions, while the intensity of these lightning strikes are found to be strongest along the coastal regions and Bay of Bengal. In addition, both the lightning properties show a very strong intensification (~1-2.5% annually) across all Indian regions during 1998-2014 with the maximum trends along the coasts. Accordingly, a detailed statistical dominance analysis is performed which reveals total column water vapor (TCWV) to be the dominant factor behind the intensification in lightning events, while instability, measured by the convective available potential energy (CAPE), and aerosols optical depth (AOD) jointly control the lightning frequency trends. An increase in surface temperatures has led to enhanced instability hence stronger moisture transport to the upper troposphere lower stratosphere regions especially in the along the coasts. This transported moisture helps deplete the ozone concentration leading to reduced temperatures and elevated equilibrium levels which finally results in stronger and more frequent lightning events as also evidenced from the trend analysis. Consequently, the relationship between lightning and its causative factors have been expressed in form of multi-linear regression equations which are then employed on multiple global circulation models (GCM) to understand the long-term impact of urbanization on lightning over a period of 1950-2100. The analysis reveals a uniform increase in lightning occurrences, and intensity from both urbanization scenarios; however, an accelerated growth is observed in the RCP8.5 projections after the year 2050 as also observed from the surface warming trends. As a result, lightning frequency and intensity values across the Indian region are expected to increase alarmingly by ~10-25% and 15-50%, respectively, by the end of this century with highest risks along the coasts and hence it requires immediate attention from policy makers.

Keywords: Lightning; occurrences; intensity; CAPE; TCWV; AOD; GCM.

1. Introduction

36 Intense thunderstorm events form a very common climatic feature over the Indian subcontinent. These phenomena
37 are generally accompanied by widespread lightning, wind gusts and heavy rainfall which induce various
38 socioeconomic hazards. However, among all these by products, lightning occurrences have been found to cause
39 the greatest damage to life with a death toll of more than 2500 every year since the last two decades (Livemint,
40 2000). In addition, the recent years have witnessed some most severe lightning calamities as per available records
41 claiming more than 100 lives on 25 June 2020 (Washington Post, 2020).

42 Over the tropics, the non-inductive (collision based) charging interaction between ice crystals and graupel
43 particles is found to be the major factor behind the evolution of lightning events during typical thunderstorms
44 (Takahashi, 1978; Mansell and Ziegler, 2013). According, in this mechanism, the magnitude of charge generated
45 per collision depends on the relative velocity of the colliding particles, the hydrometeor concentration of graupel
46 and ice and their corresponding size distributions (Shi et al., 2015) and these in-turn are controlled by the
47 atmospheric moisture content (total column water vapour), thermodynamic instability (convective available
48 potential energy) and the possibility of cloud nucleation from aerosols. Additionally, Kumar and Kamra (2012)
49 suggested that orographic lifting also has good influence on lightning but only in limited high-altitude regions of
50 Indian Subcontinent.

51 Lightning flashes are found to be significantly correlated with convective rain, total column water vapour
52 (TCWV), or surface relative humidity over both land and sea regions, according to previous studies (Price and
53 Federmesser, 2006; Siingh et al., 2011; Shi et al., 2018). This is because, higher humidity levels lead to stronger
54 hydrometeor concentration and updraft velocities, both of which contribute to intense lightning. Next, high values
55 of instability represented by convective available potential energy (CAPE) are essential for lifting the available
56 moisture with strong updrafts above the freezing level where they form ice and graupel particles which collide to
57 initiate charge separation and lightning and this has already been demonstrated both theoretically and statistically
58 in various previous research attempts (Galanki et al. 2015, Saha et al., 2017; Dewan et al. 2018).

59 Finally, coming to the impact of aerosols (AOD), a study by Shi et al., (2020) reported that the lightning
60 flash rates are strongly correlated when $AOD < 1$ due to the cloud/ice condensation nuclei formation characteristics
61 from sulphates (Jin et al., 2018), desert dust (Boose et al., 2019) or even sea salt aerosols (de Leeuw et al., 2011).
62 On the other hand, when $AOD > 1$ then normally, larger concentrations of cloud condensation nuclei result in more
63 supercooled droplets leading to stronger lightning (Williams and Stanfill, 2002). However, excessively high
64 aerosol concentrations may also result in reduced cloud droplet size (Twomey et al., 1984) which reduces the
65 efficiency of non-inductive charging process. In addition, an excess of absorptive aerosols (such as black carbon)
66 warms the atmosphere and cools the surface (Kar et al., 2009; Talukdar et al., 2019) which further reduces the
67 CAPE and lightning. Hence the reported relationships between lightning and aerosols is still unclear so, further
68 studies are required to unravel it (van den Heever and Cotton, 2007).

69 Now from climatic point of view, a series of studies in recent years have shown that thunderstorm severity,
70 lightning and its various controlling factors have been increasing prominently in the recent decades and this has
71 been attributed to greenhouse emission induced surface warming effects both over India as well as across the
72 globe. A study by Shindell et al. (2006) depicted that a minimum 10% increase in lightning activity can be
73 expected due to every 1°C increase by global warming. Kandalgaonkar et al. (2005) suggested that a rise of 1°C
74 in surface temperature over India has led to a 20–40% enhancement in average lightning flash density. According

75 to Riemann-Campe et al. (2009) and Prein et al. (2017) a recent increase of temperature has led to a rise in moisture
76 ingress, consequently the frequency and severity of intense convective activities have shown a steep rise globally.

77 Over India, Murugavel et al. (2012) and Chakraborty et al. (2019) showed a systematic increase in CAPE
78 which was attributed to thermodynamic instability conditions and large-scale dynamics coupled with a decrease
79 in upper tropospheric temperatures during that period. Also, satellite measurements have shown a prominent
80 increase in aerosol concentrations over Asia due to the intense growth in urbanization and industrialization
81 (Massie et al., 2004). Consequently, a new set of research attempts have tried to express lightning and
82 thunderstorm severities in form of their causative factors which are employed on global climate models (GCMs)
83 to provide future projections of extreme events (Diffenbaugh et al., 2013). Romps et al (2014) expressed the
84 lightning flash rate in terms of the product between CAPE and precipitation rate which when implemented on 8
85 climate models revealed an increase in lightning by $12\pm 5\%$ per degree Celsius of warming over the USA. Later,
86 a range of other proxies were also used over GCMs for lightning projections, but all of them also provided a
87 similar increase in lightning both globally as well as over the USA (Bannerjee et al., 2014; Romps, 2019).
88 However, as already hinted by Michalon et al., (1999), many years ago, most of the modelling attempts are
89 expected to fail in providing a holistic understanding about the changing lightning climatology; and interestingly
90 this is also found true at present as evidenced from major disagreements in magnitude of the projected trends
91 among all the above-mentioned studies.

92 With reference to the previous sections, it has been understood that first, a very few studies on lightning has
93 been done on the tropics and especially over the Indian region (Pereira et al., 2010) and none of the remaining
94 attempts have tried to depict the future projections of lightning. Second, all the above-mentioned studies have
95 utilized very poor resolution lightning datasets and hence did not provide a holistic mechanism behind the
96 climatological variations in lightning evolution. Finally, none of these attempts have tried to see the variation of
97 lightning radiance or intensity which is expected to be much more connected with the underlying physical
98 processes compared to the frequency values. Thus, in the present study, high resolution lightning datasets of
99 frequency and intensity are used over the Indian region and an attempt is made to identify the most dominant
100 factors affecting the spatial-temporal variabilities of the lightning properties in a complete manner. Finally, the
101 results of this dominance analysis are expressed in the form of a multi-variate regression analysis and subsequently
102 applied on multi-model GCM datasets to generate reliable future projections of lightning occurrences and intensity
103 over Indian for next few decades subject to various urbanization scenarios.

104 The main organization of the paper is explained as follows. A detailed illustration of the various datasets
105 used in this study are elaborated in the datasets section. Next comes the results section which is again divided into
106 four subsections. The first two subsections discuss the spatial distribution of lightning and its 17-year trends and
107 they also try to identify the dominant factors responsible for the multi-decadal changes in lightning. In the next
108 part, a probable physical mechanism is proposed to relate how the recently accelerated global warming trends can
109 modulate the climatic intensification and abundance of lightning. However, the final subsection tries to implement
110 the above-mentioned hypothesis on multiple long-term global climate model datasets to provide reliable future
111 projections of lightning intensity and occurrence subject to various degrees of urbanization. In the final section of
112 the manuscript, all the results have been summarized to produce a simplified picture which tries to quantify the
113 long-term impacts of global warming on lightning extremes over the Indian region for future policy makers.

114

115 2. Datasets used

116 Lightning observations for the present study are obtained from Lightning Imaging Sensors (LISs) onboard the
117 Tropical Rainfall Measuring Mission (TRMM) satellite which orbits the earth at 350 km elevation between 35°
118 N and 35°S at a rate of 16 orbits/day (Christian et al., 2003). These LISs can detect both intra-cloud and cloud-to-
119 ground discharges irrespective of day or night conditions with a flash detection efficiency of 73 ± 11 % and $93 \pm$
120 4%, respectively (Boccippio et al., 2002). The lightning observations are done by monitoring illumination pulses
121 along the 777.4 nm atomic oxygen multiplet with a very fine spatial (5.5 km) and temporal (2 ms) resolution.
122 Every time an illumination pulse registers intensity greater than the predefined background noise level, it is
123 considered as a separate lightning event after which all such events occurring within an integration time of 330
124 ms are collectively considered as a single lightning flash. The view times of these flashes are also recorded
125 separately for obtaining the monthly flash rate climatological datasets. Here it may be noted that most of the past
126 researches have used pre-processed monthly averaged lightning flash rates after 2.5° and 99-day smoothing of the
127 actual data which may have compromised the actual distribution of lightning properties in those cases. Hence, in
128 this study, the actual lightning observations from ~95800 satellite passes have been utilized during the total
129 availability period of 1998-2014. These lightning flash (/km²) datasets are compiled monthly and then averaged
130 annually while the lightning radiance values (J/m²/steradian/s⁻¹) are averaged directly on a yearly basis so that the
131 magnitudes of both these parameters remain along the same scale of 0-1 for simplicity in analysis. However, for
132 ease of region-wise analysis, the yearly time series of both these parameters has been analysed on a fixed grid
133 resolution of 1 degree.

134 While utilizing the lightning radiance measurements from satellite observations, it may be best suited to
135 explain the importance of this data towards weather and climate as this attribute has never been extensively
136 discussed in past research attempts unlike lightning frequency or flash rate. It is well known that lightning
137 activities originate due to charge separation in mixed phase clouds, but they require a sufficient amount of
138 electrostatic charge to shatter the insulation capacity of the atmosphere and descend to the earth surface thereby
139 causing widespread damage to life and property. However, a majority of these lightning occurrences are not strong
140 enough and hence they remain as intercloud lightning without any real impact on the climate or socio-economy.
141 On the other hand, according to some novel studies like Uman (1986) only 10-20% of the total lightning activities
142 remain strong enough to reach the ground thus inflicting widespread socio-economic impacts. Consequently, the
143 climatological variation of lightning intensity or radiance also needs to be monitored very closely by present
144 policy makers in order to prevent the chances of any impending catastrophises in future.

145 Next, the gridded datasets of the causative meteorological factors namely CAPE and TCWV are utilized
146 from the Climate Forecast System Reanalysis (CFSR) developed by NOAA's National Centre for Environmental
147 Prediction (NCEP) (<http://nomadl.ncep.noaa.gov/ncep-data/index.html>) datasets (Kalnay et al., 1996) as provided
148 by the ESRL PSD during the period 1948-2014. These datasets are provided at a coarse spatial resolution of 2.0°
149 × 2.0° for CAPE and 2.5° × 2.5° for TCWV, hence it had to be interpolated to 1° resolution and averaged yearly
150 for subsequent analysis. Secondly, the datasets of aerosol content (AOD) over the maximum availability period
151 of 2000-2014 are obtained from Level-3 (L3) MODIS TERRA Atmosphere Monthly Global Product MOD08_M3
152 at 1X1 grid resolution (Platnick et al., 2015) over the Indian sub-continent. Further details can be obtained
153 herewith (http://gdata1.sci.gsfc.nasa.gov/daac-bin/G3/gui.cgi?instance_id=aerosol_monthly). Gridded altitude
154 datasets at 0.25° resolution are taken from GMTED2010 global digital elevation model under TEMIS project

155 (Danielsen and Gesch, 2011). Finally, the future projections of lightning properties for various urbanization
156 scenarios are derived using gridded datasets of the temperature, humidity and ozone profiles with aerosol optical
157 depth at 550 nm from 11 general circulation models (GCMs) in the Coupled Model Inter-comparison Project
158 (CMIP5) archive (website: <http://cmip-pcmdi.llnl.gov/cmip5/>) during 1950-2100. Further details of these datasets
159 have been provided in Taylor et al. (2012) and also in subsequent sections of this study.

160

161 **3. Results and Discussion**

162 **3.1. Spatial distribution of lightning properties**

163 The climatological average of lightning frequency shown in Figure 1(a) depicts much higher values over the land
164 regions compared to Arabian Sea (AS) and Bay of Bengal (BoB). This is due to occurrence of stronger sensible
165 heat fluxes over the land regions resulting in stronger updrafts, and hence more lightning (Kumar and Kamra
166 (2012). The highest magnitude is observed along the foothills of Himalayas (72-95°E) which implies the effect of
167 orographic convection on lightning events. In these regions, the high values of lightning flashes are found
168 associated with the occurrence of a mountain breeze front during the afternoon hours (Boeck et al., 1999). The
169 secondary spatial maximum of lightning is observed along the coastline which can be attributed to widespread
170 moisture advection from the adjoining seas (Kumar and Kamra, 2012).

171 The BoB experiences moderately high lightning frequencies due to high seas surface temperatures (SSTs)
172 (above a critical threshold of 28°C according to Gadgil et al. 1984) which lead to frequent cyclonic storms and
173 lows in this region. However, AS experience lower lightning frequencies due to lower SSTs in this region (Kumar
174 and Kamra, 2012). Next, low lightning frequencies are observed along the peninsula due to reduced moisture
175 supply as it is geographical bounded by mountainous terrain along the coasts from both sides. In addition,
176 moderately high lightning frequencies are observed along the Indo-Gangetic plains (IGP) which can be due to the
177 complex interactions among the moderate moisture supply from BoB, local instability and the CCN effects from
178 transported (Boose et al., 2019) and emitted aerosols. Finally, very low values of lightning occurrences are seen
179 over West Central India (WCI) which can be due to dearth of moisture supply despite the contribution from
180 transported dust aerosols here.

181 Contrary to the occurrence climatology, the lightning radiance values (Fig. 1b) are much lower over majority
182 of land regions which is solely because of higher values of moisture content over the coastal regions leading to
183 more graupel (ice and hail particles concentrations above the freezing layer) as shown in Murugavel et al., 2012.
184 Yet, the maximum values of radiance are observed exactly along the coastline regions which reduce gradually as
185 one move further into the seas. This indicates the importance of thermal land-sea contrast which results in strong
186 moisture advection from both land and sea breezes along the land-sea boundary (Pielke, 1974) resulting in more
187 hydrometeors hence largest radiance. However, the presence of giant CCN marine aerosols particularly in AS (de
188 Leeuw et al., 2011) may also act as a secondary factor. Nevertheless, AS still experiences lower lightning radiance
189 than BoB probably due to its local meteorological factors as described earlier. Next, the lightning radiance values
190 are found distinctly lesser over PI, WCI and HIM as they receive much less moisture than the rest of India. In
191 Addition, a secondary maximum of radiances is observed over the IGP due to moderate moisture supply and
192 aerosols which can act as potential ICN/CCN thereby increasing the number of colliding hydrometeors for more
193 lightning radiance.

194 So, based on these spatial distributions of lightning occurrence and intensity, a group of 7 regions are
195 proposed for further analysis as depicted in Fig 1d. The two coastlines share high lightning occurrences as well as
196 intensity hence are referred as Coasts. Second comes PI as a landlocked region between the Coasts with moderate
197 values of both lightning properties. Region 3 and 4 are taken for both sea regions namely BoB and AS as their
198 response to lightning occurrences and radiances are quite different. Next, the Himalayan foothills are considered
199 to observe the effect of orographic convection on lightning properties independently. Then, IGP is selected since
200 it experiences quite high lightning occurrences and intensity due to complex aerosol, instability and moisture
201 interactions. Finally, WCI a remote inland region is considered as it experiences lower lightning properties due to
202 meagre moisture supply despite an important contribution from land heating and aerosols.

203 The climatologically averaged distributions of lightning frequency and intensity along with 4 most potential
204 factors influencing them (TCWV, CAPE, AOD and Altitude) for different regions are shown in Fig. S1. For
205 lightning frequency, the mean and percentiles are highest in HIM and lowest in PI and AS. However, the extreme
206 values for the Coasts and WCI are found to be higher than HIM because of frequent cyclonic and low-pressure
207 systems prevalent in these regions (Fig S1a). The Lowest lightning frequency is observed over AS. The radiance
208 and CAPE follow similar variability i.e., higher values are observed over BoB and Coasts due to more moisture
209 availability and thunderstorm occurrences while the other regions experience low to moderate values (Fig. S1b).
210 Yet a lot of extremes are observed in IGP and WCI which implies that the occurrence of surface heating lead to
211 higher cloud base heights and more ice-phase hydrometeors; hence more lightning in these regions as also
212 supported from previous studies (Price, 2009; Shindell et al., 2006).

213 The total moisture content (TCWV) is found to be highest along the Coasts and adjoining sea regions as
214 from lightning occurrences and intensity. Incidentally, the remote inland locations like PI and WCI receive much
215 reduced moisture supply which is the primary reason behind the lower lightning radiances in those regions. Next,
216 the IGP and WCI regions show highest values of AOD due to dust transport from Thar and Sahara deserts along
217 with large scale emission from various anthropogenic activities which have very complex impacts on convection.
218 Likewise, the Coasts also receive moderate aerosol supply from the adjoining seas as already described before
219 which further support lightning formation. The HIM region depicts the highest altitude variation among all the
220 regions, of which a significant fraction is present above 4 km height thereby supporting widespread orographic
221 lifting induced lightning activities. Next, PI and IGP exhibit an infinitesimally small altitude variation (<500 m)
222 which may not be sufficient to support any orographic convection. Whereas in WCI, the altitude ranges are
223 considerably higher which in turn provides a small but vital contribution towards lightning as also supported from
224 various past research attempts (Barros et al., 2004).

225 **3.2. Temporal variation of lightning properties**

226 **3.2.1. Long-term trends in lightning frequency and intensity over the Indian region**

227 The 17-year time series variations of mean annual lightning frequency and radiance are depicted for seven regions
228 and entire India in Fig. S2 along with their respective standard error values. Robust-fit regression analysis is
229 employed to study whether there are any statistically significant trends in the lightning frequency and radiance.
230 At the same time, a detailed description regarding the yearly % trends of lightning properties and their controlling
231 factors (TCWV, CAPE and AOD) are depicted along with their corresponding correlation coefficients in Fig. 2.
232 The trends of lightning frequency are found to be the highest over the Coasts, BoB and AS (with a total increase

233 of ~30%) with reasonably high correlation coefficient values which again can be attributed to an increase of both
234 moisture content and instability in these regions. However, the other regions depict much weaker values of both
235 these quantities. Here it is interesting to note that IGP depicts much weaker lightning trend which may be due to
236 the complex aerosol interactions as explained before. But in total, India has faced ~25% increase in lightning
237 frequency (with very high correlation values) in these 17 years which is alarming and hence will be discussed in
238 detail later in the study.

239 The mean annual lightning radiances show gradually increasing trends (with a total increase of ~20%) in
240 almost all regions. However, the magnitudes of % trends as well as the correlation coefficients are much lesser
241 compared to lightning frequency which implies that average radiance may not be a suitable parameter to
242 investigate the future variations in lightning. It is known that, TRMM observes both cloud-cloud and cloud-ground
243 types of lightning strikes together and out of the total, only the strongest 10% of the total strikes are intense enough
244 to reach the ground in the tropics (Uman, 1986) and cause immense damage to life and property (Holle et al.,
245 2019). Now, since it is more important to understand the trends of these extreme cases only, hence the regional
246 trends of 90th percentile of lightning radiances is examined (Fig.2a). The trends depict a very prominent all-India
247 trend of ~30% with higher correlation values compared to mean lightning radiance (Fig.2b). Additionally, the
248 coastal and sea regions depict much higher trends (>40%) than the rest of India which is extremely alarming for
249 policy makers at present. However, HIM has not shown any change in lightning radiance which may due to the
250 marginal increase in TCWV and CAPE there.

251 Further, it is investigated whether the proposed 90th percentile of radiance also agrees well with the
252 distribution of mean radiances over every Indian region; hence the corresponding values of both the quantities for
253 a total span of 68 seasons in 17 years are shown in Fig. S3. The figure depicts that the south Indian regions namely:
254 BoB, Coasts, PI and AS (with stronger maritime influence) exhibit prominent correlation values between the two
255 groups and the average ratio between the two is ~1.2; with a minimal amount of spreading which indicates that
256 there are no external factors affecting the average radiance distribution. But the northern inland zones depict a
257 prominent scattering between the groups (especially in IGP) and the ratio between them is also much higher (~1.4)
258 which indicates that some external factors such as aerosols may also exert an additional impact in intensifying the
259 radiance values well above the average radiance distributions. But overall, a good agreement is seen between the
260 lightning radiance groups thereby supporting the suitability of using p90 radiances only in the subsequent sections.

261 Next, the trends of TCWV (Fig. 2a) depict uniform trends (0.3% yearly or 5% in total) across all regions
262 with decent correlation values everywhere except HIM which are caused by prominent GHG induced global
263 warming in the recent decades as shown in previous studies. CAPE which represents the atmospheric instability
264 is the main reason for lightning evolution, hence this parameter also depicts strong interzonal variability like
265 lightning. The Coastal regions and seas experience much stronger increase of ~9% in 17 years implying more
266 thunderstorm activity in the present due to prominent global warming induced land sea thermal contrast. However,
267 the rest of the country exhibits a much weaker increase (~5%) and further, the trends in IGP and WCI are even
268 lower due to the complex aerosol effect. Finally, AOD is found to increase most significantly throughout India
269 compared to the other parameters, however the south Indian maritime regions experience a much lower rise of
270 ~25% compared to deep inland regions (WCI and IGP) with ~40% increase indicating that aerosols may have
271 more dominant role in modulating the trends of lightning properties only in the continental North Indian regions.

272 **3.2.2. Investigation of the dominant factors affecting the lightning trends over India**

273 The previous sections depict a series of spatially varying complex interactions among TCWV, CAPE and AOD
274 which resulted in an increasing trend in both lightning properties over the Indian region. Now, to identify the most
275 dominant factors affecting the trends of lightning, a clustering analysis is done for each Indian region. Hence the
276 datasets of lightning are taken for 15 years span (as AOD data is absent before 2000) and then they are sorted into
277 three clusters based on magnitude. The mean and deviation of these clusters are depicted in Fig. S4 and Fig. S5
278 with respect to corresponding values of TCWV, CAPE and AOD. Factors having dominant influence are
279 identified as those where the parameter mean increases sharply with the clusters with minimal mutual overlapping.

280 The analysis revealed that CAPE and AOD depict good clustering for occurrences while TCWV shows the
281 best results for radiances over Coast and BoB. AS also behaves similarly, but in case of occurrences, AOD fares
282 slightly better than the others implying a dominant contribution from CCN forming marine aerosol transport in
283 this region. PI experiences lesser moisture ingress (due to its inland location) hence it relies more on dry
284 convections which makes CAPE the major governing element for both the lightning properties. No single factor
285 is observed to be dominant factor for lightning frequency in HIM as it mainly relies on orographic convection
286 processes as already explained in preceding sections. But for radiance, TCWV still remains a dominant factor
287 (Fig. S5). Next in case of IGP, CAPE exhibits fair linear clustering in occurrence while TCWV remains
288 dependable for intensity. WCI behaves similar to PI but, here a secondary influence of AOD is also observed
289 indicating the possible impact of transported dust (acting as ICN) which catalyses the formation of ice phase
290 hydrometeors leading to more frequent and stronger lightning events.

291 Next, the clustering analysis is performed over the entire Indian region and is shown in Fig. 3. Based on
292 clustering and correlation analysis for lightning frequencies, CAPE emerges as the dominant factor followed by
293 AOD. This can be supported theoretically as the generation of lightning events only requires the availability of
294 ice phase hydrometeors above the freezing level which is achieved mainly by the lifting mechanism due to CAPE
295 followed by the aerosol CN effect. On the other hand, in case of p90 radiance, based on clustering and correlation
296 coefficients TCWV emerges as the single dominant feature behind the strong rise in lightning radiances all over
297 India. This result can also be explained theoretically as the inductive/non-inductive charging density responsible
298 for lightning radiance is far more dependent on the local hydrometeor concentrations (arising from moisture
299 abundance) compared to their relative vertical velocities (controlled by CAPE). Now interestingly, AOD has
300 consistently maintained a complex secondary impact on both the lightning properties depending its tendency to
301 either favour lightning (by creating more ICN/CCN formation due to dust or sulphate aerosols) or negatively by
302 inducing cloud burn-off effect(due to black carbon aerosols) as already discussed in preceding sections. So, a
303 detailed study needs to be done to untangle the AOD effect in aerosol sensitive zones like IGP and WCI.

304 Now, the temporal dominance analysis is repeated quantitatively using a multi-linear regression analysis. In
305 this step, two equations are hypothesized where lightning frequency and radiance are expressed separately as a
306 multi-linear addition of all three controlling factors. The proposed equations can be expressed as:

$$307 \text{ Lightning frequency} = a_1 * \text{TCWV} + b_1 * \text{CAPE} + c_1 * \text{AOD} \quad (1)$$

$$308 \text{ \& Lightning intensity} = a_2 * \text{TCWV} + b_2 * \text{CAPE} + c_2 * \text{AOD} \quad (2)$$

309 Here, a, b and c represent the corresponding Multiple linear regression (MLR) coefficients for the three
310 factors and the numbers 1 and 2 stands for lightning frequency and radiance, respectively. The corresponding
311 variation of these MLR coefficients is shown in Fig. 4. CAPE acts as most dominating factors in all the regions
312 expect over AS where AOD influence is very high. AOD is the second most controlling parameter in lighting

313 frequency (except over BOB and HIM). For radiances, the TCWV is the dominant factor in most regions (except
314 over PI and WCI). The reasons for this were discussed in previous section. Again, similar to AS, AOD plays the
315 most significant role in modulating both the lightning properties over IGP due to the role of complex aerosol-
316 cloud interactions.

317 Finally, over the Indian region, TCWV arises as the dominant parameter controlling the climatic trends of
318 radiances; however, for occurrence it is not so simple. Though CAPE manages to be the principal factor, yet the
319 relative contributions of AOD followed by TCWV cannot be neglected. Next, the applicability of the proposed
320 MLR equations for long-term studies are validated by showing the ratio between regressed and observed lightning
321 properties (Fig4 i & j). In case of occurrences, the ratio between the two is not perfect and a small overestimation
322 of ~5% is observed hence this bias has been corrected before using it in the coming sections. Whereas, the
323 regressed values of radiance match perfectly with observations. Henceforth, these MLR equations have been
324 utilized for deriving the reliable long-term projections of lightning properties in subsequent sections.

325 **3.3 Physical mechanisms driving the increasing trends in lightning properties**

326 In this section, the physical processes responsible for the increase in lightning occurrences and intensity over the
327 Indian region will be discussed. Recent studies showed a prominent increase in aerosols and GHG emissions over
328 the Coasts, IGP and WCI as seen from the very strong increase in AOD in the recent years. This phenomenon
329 resulted in widespread surface and atmospheric warming (Basha et al. 2017) and consequently a stronger surface
330 evaporation and moisture production. In addition, many recent research attempts have reported a net increase in
331 the Hadley cell and Brewer–Dobson circulation strength (Liu et al., 2012; Fu et al., 2015), which also assists in
332 additional moisture supply. Consequently, the increased moisture in the atmosphere further accelerated the
333 warming effect and TCWV growth in forms of a positive feedback (IPCC, 2007) primarily in the Coastal and
334 neighbouring sea regions like BoB and AS. However, the increased moisture supply in IGP or PI is mainly due to
335 the enhanced land-sea thermal contrast effect (due to GHG and aerosol emissions) which intensifies the moisture
336 converges in these regions.

337 To explain how thermodynamic instability or CAPE has been increasing recently, a previous study by
338 Chakraborty et al. (2019) is referred where long-term multi-station radiosonde observations depicted strong
339 increasing trends in CAPE and TCWV all over Indian region with the maximum values along the coasts and
340 surrounding inland regions. However out of the total column, the percentage trends in both instability and
341 moisture integrals (CAPE or TCWV) are found to be particularly higher above 300 hPa pressure levels which can
342 be associated with a gradually ascending level of neutral buoyancy (LNB/EL) during this period. Now as the EL
343 comes very close to the 100 hPa level during intense convective events, hence an observed cooling at its immediate
344 surroundings (135-95 hPa) is thought to be the main factor responsible for the EL ascent and CAPE increase in
345 these regions. The main reason for considering this hypothesis is based on a study by Dhaka et al. (2010) where
346 a very prominent anticorrelation was observed between the yearly average values of CAPE and their
347 corresponding upper-tropospheric temperatures at 100 hPa.

348 It has been well documented in past studies that ozone molecules act as the primary heat source component
349 at 100 hPa level (corresponding to the UTLS region) by absorbing the ultraviolet radiations (Mohankumar, 2008).
350 Now, the multi-station radiosonde observations from Chakraborty et al. (2019) depicted a clear rise in specific
351 humidity and a depletion in ozone mixing ratios at the same height range. These results were analogous with the
352 findings from Forster et al. (2007) according to which the recent decades have experienced an upper tropospheric

353 cooling due to a decrease in ozone concentration. Thus, a cooling trend at this height level can be explained by
354 the theory that excess moisture pumped to this height by intense convections get disassociated photolytically by
355 reactive oxygen atoms to produce two OH radicals which further decompose ozone to oxygen molecule and a
356 reactive oxygen atom in the UTLS region (Guha et al. 2017) thereby continuing the process. Consequently, this
357 feedback process would lead to a further ascent in EL and increase in CAPE; however, the magnitudes of the
358 resultant CAPE intensification will be highest over the coasts and surrounding seas due to a stronger moisture
359 advection in those regions.

360 Hence according to this hypothesis, the Coastal regions and seas experience more growth in TCWV and
361 CAPE which lead to formation of more ice phase hydrometeors thereby promoting an accelerated rise in lightning
362 radiance. On the other hand, larger CAPE favours more updraft velocities in the ascending particles which further
363 increase the probability of hydrometeor collisions leading to an increased lightning frequency. However, an
364 additional effect can also be cast by AOD by facilitating more CN formation (from dust, sulphate or sea salt
365 aerosols) which will strengthen the above-mentioned physical mechanism thereby leading to a stronger increase
366 in both lightning properties over the aerosol sensitive inland regions such as IGP, WCI and PI.

367 **3.4 Generation of reliable future projections of lightning frequency and intensity**

368 **3.4.1 Selection of GCMs for future projection analysis**

369 In this section, the MLR coefficients from previous sections are employed to provide reliable projections of future
370 lightning activities over the Indian region. Accordingly, the datasets of CAPE, AOD and TCWV are utilized over
371 a period of 150 years including first 55 years (1950-2005) from historical datasets and the rest (2006-2100) from
372 two extreme future scenarios namely: RCP2.6 and 8.5. A set of 8 global climate models (GCM) of CMIP5
373 (depicted in Table S1) are selected for analysis as all of them commonly provide the monthly mean estimates of
374 TCWV and AOD with daily profiles of temperature, humidity and ozone. The monthly average values of CAPE
375 are then calculated from daily T and RH profiles using the parcel approximation technique as described in past
376 research attempts (Chakraborty et al., 2018; Narendra Reddy et al., 2018). It may be noted that, the surface-based
377 CAPE (SB-CAPE) calculation technique has been used to obtain the current CAPE values in this study since they
378 measure the total buoyancy experienced by the parcel raised directly from the surface to any height of the
379 atmosphere irrespective of the prevailing atmospheric conditions, seasonality or the region where it is being
380 derived. Now, the datasets from each of these models are interpolated to a uniform 1X1 degree resolution after
381 which their performances are tested by comparing the simulated CAPE, TCWV and AOD values with respect to
382 NCEP NCAR reanalysis datasets. The results of this test are represented in terms of a Taylor diagram in Fig. 5.

383 The Taylor diagram results for TCWV, CAPE and AOD unanimously reveal that models ACCESS1.3
384 CSIRO MK3.6, MIROC5 and NOESM 1ME (represented as A, B, F and H in Fig.5.) depict good correlations
385 over the Indian region along with lower std and rms values. In addition, the model derived monthly inputs are also
386 validated against NCEP data for all seven regions in Fig. S6. The correlation coefficients for all regions commonly
387 show that models ACCESS1.3 CSIRO MK3.6, MIROC5 and NOESM 1ME again show much better agreement
388 with NCEP data. Hence these four models are considered further for lightning projection analysis. Next, the all-
389 India averaged regressed lightning occurrences and intensity values obtained from the models during 2000-2014
390 are plotted against their corresponding observations to check the reliability of MLR analysis on the modelled data.
391 The results depict a fair agreement between the two sets ($r=0.76$ in occurrences and 0.7 in radiance) in both the

392 cases. However, a very prominent underestimation bias has been observed (~24% in occurrences and ~18% in
393 radiances) which is probably because the modelled datasets are of much coarser resolution than the actual
394 observations, hence they will always depict much lesser average or variability compared to the former. However,
395 the inter comparisons between the modelled and observed lightning properties over all the regions commonly
396 depict quite high values of correlation with an overall underestimation bias of 17-25% thereby supporting the
397 reliability of MLR analysis. However, the underestimation biases obtained from inter-comparison tests must be
398 added with the regressed climatic projections for both zonal and all-India cases to get the actual lightning trends
399 in forthcoming sections.

400 **3.4.2 Examination of the 150-year trends in various factors controlling lightning**

401 The 150-year trends of various controlling factors associated with the climatic trends of lightning occurrences and
402 intensity are shown in form of normalized % change per decade for all seven Indian regions in Fig. S7. The surface
403 temperature trends are first considered as this parameter is closely associated with urbanization and GHG
404 emissions and it also acts as the primary driver behind the CAPE and TCWV trends. A moderate rise in RCP2.6
405 is observed (~0.5% per decade) which represents an all-India warming by ~1.6°C in total while the RCP8.5
406 scenario exhibits an extremely severe warming of ~5°C in the Coasts, WCI, BoB and IGP which is also expected
407 to cause a parallel increase in TCWV and CAPE in future. Next, at par with surface warming, TCWV exhibits a
408 moderate increase from RCP2.6 scenario but in case of RCP8.5, an alarming growth of ~40% is observed across
409 India (with the largest increase in the Coasts, BoB and AS) which will definitely lead to a parallel huge change in
410 extreme lightning radiances over the total span of 150 years.

411 In case of AOD, contrary to the extremely large increase of ~30-40% between 2000 and 2014 from MODIS,
412 a much smaller rise of only 20% is seen during a much larger span of 150 years. Now to understand the source of
413 this discrepancy, the 150-year time series of AOD is observed which reveals that the initially increasing trend of
414 aerosols reverses to a strong negative trend after 2020 which results in an overall weak positive trend. The sudden
415 decline in AOD can be explained by the fact that RCP2.6 scenarios are characterized by stringent control on GHG
416 emissions and aerosols after 2020. However, RCP8.5 scenarios exhibit a higher overall increasing trend
417 amounting to 60%. Now this improvement in AOD trend from the latter case is because after 2020 the AOD
418 values saturates and then it shows a weak negative trend implying minor aerosol emission restrictions in future;
419 hence, the net cancellation of trends does not happen here. Also, the net increase in AOD is moderate in the Coasts
420 but much higher in aerosol sensitive regions like IGP and WCI implying even a doubling of AOD in these regions
421 which again may cast some vital influence on the lightning frequency trends of these regions in future.

422 Next in accordance with the TCWV and temperature trends, CAPE and MLCAPE depict a 15% and 8%
423 increase in total from RCP2.6 scenarios. Also, the CAPE trends are much higher than in MLCAPE which indicate
424 the validity of the upper tropospheric intensification theory as explained earlier. Again, the trends in CAPE and
425 MLCAPE are the highest being over Coasts and surrounding regions due to maximized moisture availability as
426 also shown in the previous studies. However, the RCP8.5 scenario shows an alarmingly high total trends of ~50%
427 and 20% in CAPE and MLCAPE respectively due to intensified global warming and moisture availability with
428 the highest rise of ~60% over the Coasts and seas which implies the possibility of accelerated growth in lightning
429 occurrence in these zones. However, inland regions (IGP and WCI) still show moderately high CAPE trends (due
430 to strong surface heating and aerosol trends) which may also lead to stronger lightning frequencies there.

431 Next, the trends in EL pressure level show an expected depletion (implying an ascent in EL) from RCP2.6
432 scenario with values between 0.5-1 % hPa per decade. However, in RCP8.5, the trends are further enhanced with
433 a range of 1-2% per decade with the largest changes occurring in the Coasts and BoB followed by IGP and WCI
434 due to a stronger increase in CAPE and TCWV. Similarly, the T100 cooling trends experience exactly similar
435 behaviour as EL with ~1-degree cooling in Coastal regions from RCP2.6 scenario while in case of RCP8.5, a
436 drastic cooling of up to ~2°C is observed in total which can highly invigorate the convective strengths leading to
437 much stronger lightning events in future. Next, in RCP2.6 case, SHUM at 100 hPa undergoes ~0.3% increase per
438 decade associated with a 1% decrease in ozone. Here it may be noted that the ozone depletion trends are much
439 higher than in SHUM only because the photolytic disassociation of a single water vapour molecule with reactive
440 oxygen atom produces two OH radicals which help in decomposition of two ozone molecules. However, using
441 RCP8.5 scenario, these phenomena gets further amplified where -0.6% per decade increase in SHUM and (-2%)
442 depletion in ozone is observed with highest magnitudes observed in the Coasts. Hence the results suggest that
443 under higher surface warming (RCP8.5 scenarios), CAPE and TCWV will increase by exactly same hypothesis
444 as shown in Section 3.3 which ultimately results in a very strong increase in lightning properties over India

445 Now, coexistent with the zonal decadal trends the all-India time series of all parameters are shown in Fig. 6.
446 The surface temperatures depict an increase by 2 and 4 degrees, while the TCWV and CAPE also rise by 10%,
447 50% and 20%, 40% respectively for the two pathways. However, it may be noted that the main difference in
448 TCWV trends between RCP2.6 or 8.5 scenarios mainly arises from its drastic increase in the latter case after 2050
449 which is again attributed to the accelerated global warming conditions experienced using RCP8.5 scenarios during
450 those decades. Next, the AOD follows a dampened increasing trend in both scenarios with the increase in latter
451 being slightly more prominent than the former. Now these dampened AOD trends are expected to reduce the net
452 growth in lightning occurrences (owing to AOD's prominent contribution in the lightning frequency MLR
453 coefficients), but such effects will not be discernible in the radiance trends as it depends primarily on TCWV only.
454 Now because of the CAPE and TCWV trends, EL has shown a prominent ascent coupled with strong UTLS
455 cooling and increased moistening and ozone depletion trends in both urbanization scenarios. However, the trends
456 in RCP8.5 scenario are consistently much stronger than the RCP2.6 case due to much stronger GHG induced
457 UTLS dynamics and CAPE intensification feedback effect. In addition, the main difference between the trends
458 from both scenarios is mostly prominent towards the end of 21st century as explained previously.

459 **3.4.3 Expected overall trends in lightning frequency and intensity**

460 The 150-year trends in lightning properties for all seven Indian zones are observed in Fig. S7. The lightning
461 occurrences depict an overall increasing trend of ~15-25% for the total 150-year span which after adjustment for
462 underestimation bias (20-27% as in Fig. S6) provides the actual trends to be 19-31%. However, this increase of
463 lightning occurrences is rather low compared to the 17-year trends from observations. Hence, the lightning
464 frequency time series for each zone is investigated separately which reveal that the lightning frequencies have
465 increased up to 2020 after which it gets saturated; nevertheless after 2050, it again started to increase up to 2100
466 thereby leading to much lower trend values (Fig. 6). However, this type of variation can be explained by the
467 secondary influence of AOD on lightning occurrences which also shows a dampened increase thereby
468 compensating the impact of increasing CAPE in totality. In addition, out of all regions, the strongest increase in
469 lightning frequency is mainly observed in the Coasts, BoB, PI, IGP and WCI which is primarily due to influence
470 of CAPE and moisture supply in the first two and due to dry surface heating and aerosol effect in the rest. However,

471 in RCP8.5 scenarios, a much larger trend values amounting to 29-41% are observed (after bias correction) which
472 is mainly attributed to the stronger increase in CAPE and TCWV and a weaker decline in AOD in this case.
473 However, the spatial distribution of the trends remains fairly like the RCP2.6 case.

474 The 150-year zonal trends in lightning radiance from RCP2.6 scenarios depict a prominent overall increasing
475 trend of 35-54% after zone-specific bias corrections. Here the radiance trends are found to be much higher than
476 in occurrences since the lightning radiance trends depend primarily on TCWV which also shows a prominent
477 increase across the 150-year span. However, the net radiances are still a bit lower than the expected trends from
478 observations due to the small declining trend contribution from aerosols. However, the RCP8.5 scenario depicts
479 a very alarming increase amounting to (56-97% after bias correction) which can be attributed to the stronger
480 increase in both TCWV and CAPE throughout 150 years coupled with a weaker decline in AOD. In addition, the
481 lightning radiance trends are found to be the strongest in the Coasts and BoB, due to the accelerated rise in TCWV
482 and CAPE while a slightly weaker trend is observed over IGP and WCI due to the compensating influence of
483 AOD in addition to the TCWV and CAPE trends.

484 Now, at par with the zone-wise decadal lightning trends, the all- India averaged time series of lightning
485 occurrences and intensity are depicted in Fig. 7. The lightning occurrences from RCP2.6 scenarios depict a weak
486 increasing trend amounting to 26% (after bias correction of 24%) over the 150-year time span. As already
487 explained, the weak trend observed is due to the cancellation between increasing trends of CAPE and TCWV
488 against a declining trend in AOD. But in case of RCP8.5, a considerable increase in lightning frequency amounting
489 to 35% is observed which is mainly due to a strong rise in CAPE and TCWV along with a weaker decline in AOD.
490 In case of extreme radiances, RCP2.6 scenario shows a moderate rise of ~45% throughout India (after a bias
491 correction of 18%). However, RCP8.5 scenario depict a much higher increase by ~73% which is due to the much
492 stronger rise in TCWV followed by CAPE with minimal contribution from AOD. In addition, an exponential rise
493 in both TCWV and CAPE are observed after 2060 because of excessive GHG emission induced global warming
494 thereby leading to the highest increase in lightning radiance over India after 2060.

495 Now finally, an attempt is made to estimate the net % increase in lightning properties starting from the
496 present (2010-2020) in order to describe the probable difference in lightning trends if two extreme GHG emission
497 policies are adopted. Under these circumstances, the lightning frequencies depict a weak rise of ~13% assuming
498 RCP2.6 scenario but this trend would increase to ~19% in case of RCP8.5 while in the coasts, the trends may be
499 slightly higher reaching a maximum of ~22% for the latter. Yet, these trend values are quite smaller and hence
500 can be avoided quite easily in the future. However, in case of extreme radiance, the minimum possible increase
501 considering stringent policy making decisions from RCP2.6 scenario is ~22% throughout India. But in absence of
502 such restrictions (RCP8.5) the overall increase in extreme radiance will be ~37% with respect to present. In
503 addition, due to the impact of stronger TCWV and CAPE trends, the Coastal regions can face even up to a ~50%
504 rise in extreme lightning intensities by 2100 which poses an extreme socio-economic threat and hence requires
505 immediate mitigation strategies from policy makers at present.

506

507 **4. Summary and Conclusions**

508 Lightning activities are considered as an essential by-product of thunderstorms and they pose the greatest damage
509 to life annually since the last few decades. However, only a few studies have been reported over India or globally
510 which attempted to understand the evolution and distribution of lightning processes in overall and thereby provide

511 a reliable estimate about the future projections of lightning. Hence, the present study, attempts to utilize high
512 resolution lightning observations to explain its socio-temporal variabilities over India and also to identify the most
513 dominant factors responsible for the evolution of such extremes. In addition, the proposed inter-relationships
514 between lightning and its causative factors namely: moisture, instability and aerosols are also implemented in
515 multi-model GCM datasets to derive reliable future projections of lightning properties over the Indian regions for
516 the 21st century. The main highlights obtained from the present study include:

- 517 1. The highest climatological average of lightning occurrences is observed along the Himalayan foothills,
518 followed by coastal regions and Indo-Gangetic plains which are mainly attributed to the influence of
519 orographic convection, moisture ingress (due to land-sea thermal contrast) and aerosol cloud interactions.
- 520 2. Annual average values of lightning radiances are the strongest along the coastal regions and surrounding
521 seas primarily due to the dominance of hydrometeor concentrations on the lightning charge density equations
522 caused by enhanced moisture availability in those regions.
- 523 3. During the period 1998-2014, lightning frequencies exhibit a strong growth of ~1-2 % annually across all
524 Indian regions with a strong inter-regional variability. However, the trend values are invariant and quite
525 lower in the average radiance trends. Therefore, the trends in 90th percentile radiances are estimated which
526 show prominent spatial variation with 2-2.5% increase annually along Coasts, BOB, PI and IGP. These zonal
527 diversities in the lightning trends are also supported by the corresponding CAPE and AOD trends.
- 528 4. The clustering and multi-linear regression dominance tests depict that over India as a whole, atmospheric
529 moisture (TCWV) is the principle factor controlling the lightning extreme radiance trends, while instability
530 (CAPE) and aerosols (AOD) jointly play a strong role behind lightning frequency variation. However, in the
531 latter, the proposed inter-relationships are found to deviate from region to region due to complex aerosol-
532 cloud interactions towards thunderstorm genesis and lightning evolution.
- 533 5. Results from previous research attempts are employed to explain the underlying physical mechanism of these
534 trends which inferred that an increase in surface temperatures has led to higher instability and moisture
535 transport to the UTLS regions. This moistening resulted in ozone depletion and cooling which further
536 uplifted the equilibrium levels leading to stronger CAPE and more ice-phase collisions above the freezing
537 level; and eventually this complex feedback procedure ultimately leads to stronger and much more lightning
538 events. A schematic of these processes has been depicted in Fig. 8.
- 539 6. The above-mentioned hypothesis is found to be most prominent in the coasts and surrounding seas due to its
540 high moisture abundance. However, in addition to these factors, this mechanism will also be further
541 invigorated/inhibited based on the prevailing RCP scenarios and also depending on the region-specific
542 aerosol input on convective processes as discussed before.
- 543 7. These observed inter-relationships are expressed in form of multi-linear regression equations and then
544 implemented on 4 suitable GCMs out of 8 available models during 1950-2100. The resulting multi-decadal
545 projections reveal prominent trends in surface temperatures, moisture, instability and subsequent ozone and
546 moisture concentrations in UTLS as proposed. However, a difference in urbanization rates led to much
547 sharper trends in all parameters particularly after 2050 in the RCP8.5 case.
- 548 8. Consequently, the regressed lightning projections also depict an increase in both occurrences and intensity.
549 However, the increasing trends are consistently higher in the RCP8.5 case. In addition, the increase in
550 lightning frequency is found to be much slower than in case of intensities due to the dominant impact of

551 AOD trends which also show a comparative saturation or decrease after 2020. This can be attributed to a
552 probable increase in GHG emission restrictions by policy makers in near future.

553 9. Finally, the net intensification in lightning properties by 2100 with respect to present values depict that
554 number of occurrences would increase moderately by (10-17 % and 16-23%) for RCP2.6 and 8.5 scenarios.
555 However, extreme lightning radiances will increase much faster by 16-27% and 32-50% in RCP2.6 and 8.5,
556 throughout India.

557 10. In addition to the overall trends, certain regions like the coasts and surrounding seas are prone to be at the
558 higher lightning risk in future since they show much stronger increasing trends of ~50% (for radiance) in
559 absence of stringent GHG emission restrictions (as in RCP8.5) which is extremely alarming and hence should
560 be immediately addressed by policy makers.

561 It may be noted that this is the first ever study to use high resolution observations of lightning radiance as well as
562 frequency over the Indian region where a holistic inter-relation between lightning and its causative factors have
563 been proposed, tested and then implemented over a set of GCMs so as to provide a set of future projections for
564 both lightning properties till the end of this century. Now, the lightning projections laid out in this study can be
565 considered as reliable for forthcoming research attempts since both the equations and the models have been
566 repeatedly validated against observational datasets. Nevertheless, the projected lightning increase due to global
567 warming in this study is found to be much lesser than that obtained by simultaneous studies over the United States
568 (as evidenced from Romps (2019)), the reason for which can be possibly attributed either to stronger urbanizations
569 conditions in those regions or the choice of lightning proxies and GCM datasets used in that study.

570 However, from a closer point of view, the present study still has certain shortcomings. The primary limitation
571 is that it tries to provide an overall explanation for lightning trends over the Indian region. However, for specific
572 regions of the country such as WCI, HIM or IGP, secondary mechanisms from orographic influence or aerosol
573 effects (both radiative or microphysical) can also play a stronger role on the lightning trends and hence this
574 requires another dedicated study to address these issues. Secondly, the observed trends may vary strongly when
575 observed for separate seasons which have been averted here to provide a more focussed investigation on the
576 climatic trends of lightning. Finally, this study provides an overall mechanism of lightning; however, this
577 procedure may not be followed for all types of thunderstorm events, hence in future a suite of numerical models
578 and observations are required to explain how individual lightning events may be impacted by the complex aerosol,
579 instability and moisture interactions within the cloud over various meteorological conditions and Indian locations.

580

581 **Data availability**

582 High resolution lightning datasets for the present study have been obtained from LIS archives of NASA Global
583 Hydrology Resource Centre DAAC, U.S.A. (https://ghrc.nsstc.nasa.gov/lightning/data/data_lis_trmm.html last
584 access: 16 December 2020). Gridded datasets of CAPE and TCWV are utilized from the CFSR reanalysis archives
585 developed by NCEP (<http://nomadl.ncep.noaa.gov/ncep-data/index.html> last access: 10 December 2020). The
586 datasets of AOD are utilized from Level-3 (L3) MODIS TERRA Atmosphere Monthly Global Product
587 MOD08_M3 (http://gdata1.sci.gsfc.nasa.gov/daac-bin/G3/gui.cgi?instance_id=aerosol_monthly last access: 10
588 December 2020). Finally, the future projections of lightning properties are derived from 11 general circulation
589 models (GCMs) in the Coupled Model Inter-comparison Project (CMIP5) archive (website: [http://cmip-
590 pcmdi.llnl.gov/cmip5/](http://cmip-pcmdi.llnl.gov/cmip5/) last access: 1 December 2020).

591

592 **Author contributions**

593 RC performed complete analysis and wrote the first draft. MVR and SGB provided the initial concept and did the
594 main editing while AC contributed to supervision, discussion, and editing.

595

596 **Competing interests**

597 The authors declare that they have no conflict of interest.

598

599 **Acknowledgments**

600 One of the authors (Rohit Chakraborty) thanks the Institute of Eminence Grant and Department of Science and
601 Technology for providing support under C V Raman Post-Doctoral fellowship and INSPIRE Faculty Research
602 Grant. He also acknowledges the Indian Institute of Science, for providing necessary support for this work. AC
603 acknowledges funding from the National Monsoon Mission, Ministry of Earth Sciences, Govt of India.

604

605

606

607

608 **References**

609 Banerjee, A., Archibald, A. T., Maycock, A. C., Telford, P., Abraham, N. L., Yang, X., Braesicke, P., and Pyle,
610 J. A.: Lightning NO_x, a key chemistry–climate interaction: impacts of future climate change and consequences
611 for tropospheric oxidising capacity, *Atmos. Chem. Phys.*, 14, 9871–9881, [https://doi.org/10.5194/acp-14-9871-](https://doi.org/10.5194/acp-14-9871-2014)
612 2014, 2014.

613 Barros, A. P., and T. J. Lang.: Exploring spatial modes of variability of terrain-atmosphere interactions in the
614 Himalayas during monsoon onset, *Hydrosci. Rep. Ser. 03–001*, 51, Div. of Eng. and Appl. Sci., Harvard Univ.,
615 Cambridge, Mass., 2003.

616 Basha, G., Kishore, P., Ratnam, M. V., Jayaraman, A., Kouchak, A. A., Ouarda, T. B. M. J., and Velicogna, I.:
617 Historical and Projected Surface Temperature over India during 20th and 21st century, *Sci. Rep.*, 7, 2987, 2017

618 Boccippio, D. J., Koshak, W. K. and Blakeslee, R.J.: Performance assessment of optical transient detector and
619 lightning imaging sensor, part I: diurnal variability. *J. Atmos. Ocean. Technol.* 19, 1318–1332, 2002.

620 Boeck, W. L., Mach, D., Goodman, S. J., and Christian Jr. H. J.: Optical observations of lightning in Northern
621 India, Himalayan mountain countries and Tibet, in 11th International Conference on Atmospheric Electricity,
622 NASA Conf. Publ., NASA/CP-1999-209261, 420–423, 1999.

623 Boose, Y., Baloh, P., Plötze, M., Ofner, J., Grothe, H., Sierau, B., Lohmann, U., and Kanji, Z. A.: Heterogeneous
624 ice nucleation on dust particles sourced from nine deserts worldwide – Part 2: Deposition nucleation and
625 condensation freezing, *Atmos. Chem. Phys.*, 19, 1059–1076, h

626 Chakraborty, R., Basha, G., and Ratnam, M. V.: Diurnal and long-term variation of instability indices over
627 tropical region in India, *Atmos. Res.*, 207, 145–154, <https://doi.org/10.1016/j.atmosres.2018.03.012>, 2018.

628 Chakraborty, R., Venkat Ratnam, M., and Basha, S. G.: Long-term trends of instability and associated
629 parameters over the Indian region obtained using a radiosonde network, *Atmos. Chem. Phys.*, 19, 3687–3705,
630 <https://doi.org/10.5194/acp-19-3687-2019>, 2019.

631 Christian, H. J., Blakeslee, R. J., Boccippio, D. J., Boeck, W. J., Buechler, D. E., Driscoll, K. T., Goodman, S.
632 J., Hall, J. M., Koshak, W. J., Mach, D. M. and Stewart, M. F.: Global frequency and distribution of lightning
633 observed from space optical transient detector. *J. Geophys. Res.* 108, 4005. 2003.

634 Danielson, J. J. and Gesch, D. B.: Global multi-resolution terrain elevation data 2010 (GMTED2010): U.S.
635 Geological Survey Open-File Report 2011-1073, pp 26, 2011.

636 de Leeuw, G., Andreas, E. L., Anguelova, M. D., Fairall, C. W., Lewis, E. R., O'Dowd, C., Schulz, M. and
637 Schwartz, S. E: Production flux of sea spray aerosol. *Rev. Geophys.* 49, RG2001.
638 <http://dx.doi.org/10.1029/2010RG000349>, 2011.

639 Dewan, A., Ongee, E. T., Rafiuddin, M., Rahman, M. M. and Mahmood, R.: Lightning activity associated
640 precipitation and CAPE over Bangladesh. *Int. J. Climatol.* 38, 1649-1660. doi:[10.1002/joc.5286](https://doi.org/10.1002/joc.5286), 2018.

641 Dhaka, S. K., Sapra, R., Panwar, V., Goel, A., Bhatnagar, R., and Kaur, M.: Influence of large-scale variations
642 in convective available potential energy (CAPE) and solar cycle over temperature in tropopause region at Delhi
643 (28.3_N, 77.1_E), Kolkata (22.3_N, 88.2_E), Cochin (10_N, 77_E), and Trivandrum (8.5_N, 77.0_E) using
644 radiosonde during 1980–2005, *Earth Planets Space*, 62, 319–331, 2010.

645 Diffenbaugh, N. S., Scherer, M., and Trapp, R. J.: Robust increases in severe thunderstorm environments due to
646 greenhouse forcing, *P. Natl. Acad. Sci. USA*, 110, 16361–16366, 2013.

647 Forster, P. M., Bodeker, G., Schofield, R., Solomon, S., and Thompson, D.: Effects of ozone cooling in the
648 tropical lower stratosphere and upper troposphere, *Geophys. Res. Lett.*, 34, L23813, 2007.

649 Fu, Q., Lin, P., Solomon, S., and Hartmann, D. L.: Observational evidence of strengthening of the Brewer-
650 Dobson circulation since 1980, *J. Geophys. Res.-Atmos.*, 120, 10214–10228, 2015.

651 Gadgil, S., Joseph, P.V. and Joshi, P.V.: Ocean–atmosphere coupling over monsoon regions. *Nature* 312, 141–
652 143, 1984.

653 Galanaki E, Kotroni V, Lagouvardos K and Argiriou A.: A ten-year analysis of cloud-to-ground lightning
654 activity over Eastern Mediterranean region. *Atmos. Res.* 166, 213–222., 2015

655 Guha, B. K., Chakraborty, R., Saha, U. and Maitra, A.: Tropopause height characteristics with ozone over
656 stratospheric moistening during intense convection over Indian sub-continent, *Global Planet. Change*, 158, 1–
657 12, 2017.

658 Holle, R. L., Dewan, A., Said, R., Brooks, W.A., Hossain, M.F. and Rafiuddin, M.: Fatalities related to lightning
659 occurrence and agriculture in Bangladesh. *Int. J. Disaster Risk Reduct.*, 41, 101264, 2019.

660 IPCC TAR-07, <https://www.ipcc.ch/site/assets/uploads/2018/03/TAR-07.pdf>, 2018.

661 Jin, Q., Grandey, B. S., Rothenberg, D., Avramov, A., and Wang, C.: Impacts on cloud radiative effects induced
662 by coexisting aerosols from international shipping and maritime DMS emissions, *Atmos. Chem. Phys.*, 18,
663 16793–16808, <https://doi.org/10.5194/acp-18-16793-2018>, 2018.

664 Kalnay, E. Kanamitsu, M. Kistler, R. Collins, W., Deaven, D. Gandin, L. Iredell, M. Saha, S. White, G. Woollen,
665 J. Zhu, Y. Leetmaa, A. Reynolds, B. Chelliah, M. Ebisuzaki, W. Higgins, W. Janowiak, J. Mo, K. C. Ropelewski,
666 C. Wang, J. Roy, J. and Dennis, J.: The NCEP/NCAR 40-Year Reanalysis Project. *Bull. Amer. Meteor. Soc.*,
667 77, 437–472, 1996.

668 Kandalgaonkar, S. S., Tinmaker, M. I. R., Kulkarni, J. R., Nath, A. S. and Kulkarni, M. K.: Spatio-temporal
669 variability of lightning activity over the Indian region. *J. Geophys. Res.* 110, D11108, 2005.

- 670 Kar, S. K., Liou, Y. A. and Ha, K. J.: Aerosol effects on the enhancement of cloud-to-ground lightning over
671 major urban areas of South Korea. *Atmos. Res.* 92, 80–87, 2009.
- 672 Kumar, P. R. and Kamra, A. K.: Land–sea contrast in lightning activity over the sea and peninsular regions of
673 South/Southeast Asia, *Atmos. Res.*, 118, 52–67, 2012.
- 674 Liu, J., Song, M., Hu, Y., and Ren, X.: Changes in strength and width of Hadley Circulation since 1871, *Clim.*
675 *Past*, 8, 1169– 1175, 2012.
- 676 Livemint: [https://www.livemint.com/Politics/ZhfsGYczjwDo22DtvDKfN/Lightnings-a-bigger-killer-than-](https://www.livemint.com/Politics/ZhfsGYczjwDo22DtvDKfN/Lightnings-a-bigger-killer-than-you-think.html)
677 [you-think.html](https://www.livemint.com/Politics/ZhfsGYczjwDo22DtvDKfN/Lightnings-a-bigger-killer-than-you-think.html), last access: 19 September 2020
- 678 Mansell, E. R. and Ziegler, C. L.: Aerosol effects on simulated storm electrification and precipitation in moment
679 microphysics model. *J. Atmos. Sci.* 70, 2032–2050, 2013.
- 680 Massie, S. T., Torres, O. and Smith, S. J.: Total Ozone Mapping Spectrometer (TOMS) observations of increases
681 in Asian aerosol in winter from 1979 to 2000. *J. Geophys. Res.* 109, D18211, 2004.
- 682 Michalon, N., Nassif, A., Saouri, T., Royer, J. F. and Pontikis, C.A.: Contribution to the climatological study of
683 lightning *Geophys. Res. Lett.* 26, 3097–3100, 1999.
- 684 Mohanakumar, K.: *Stratosphere-troposphere interactions: introduction*, Springer Science Business Media, the
685 Netherlands, 2008.
- 686 Murugavel, P., Pawar, S. D., and Gopalakrishnan, V.: Trends of convective available potential energy over the
687 Indian region and its effect on rainfall, *Int. J. Climatol.*, 32, 1362–1372, 2012.
- 688 Narendra Reddy, N., Venkat Ratnam, M., Basha, G., and Ravikiran, V.: Cloud vertical structure over a tropical
689 station obtained using long-term high-resolution radiosonde measurements, *Atmos. Chem. Phys.*, 18, 11709–
690 11727, 2018.
- 691 Pereira, Felix B., Priyadarsini, G. and Girish, T.E.: A possible relationship between global warming and
692 lightning activity India during period 1998–2009. *arXiv: General Physics*, arxiv.org/pdf/1012.3338, 2010
- 693 Pielke, R.A.: A three-dimensional numerical model of the sea breezes over south Florida. *Mon. Weather Rev.*
694 102, 115–139, 1974.
- 695 Platnick, S., et al.: *MODIS Atmosphere L3 Monthly Product*. NASA MODIS Adaptive Processing System,
696 Goddard Space Flight Center, USA, 2015.
- 697 Prein, A. F., Rasmussen, R. M., Ikeda, K., Liu, C., Clark, M. P., Holland, G. J.: Future intensification of hourly
698 precipitation extremes, *Nat. Clim. Change*, 7, 48–52, 2017.
- 699 Price, C.: Will drier climate result in lightning?, *Atmos. Res.* 91, 479–484, 2009.
- 700 Price, C. and Federmesser, B.: Lightning-rainfall relationships in Mediterranean winter thunderstorms.
701 *Geophys. Res. Lett.* 33, L07813. 2006.
- 702 Riemann-Campe, K., Fraedrich, K., and Lunkeit, F.: A global climatology of convective available potential
703 energy (CAPE) and convective inhibition (CIN) in ERA-40 reanalysis, *Atmos. Res.*, 93, 534–545, 2009
- 704 Romps, D. M., Seeley, J. T., Vollaro, D and Molinari, J.: Projected increase in lightning strikes in the United
705 States due to global warming, *Science*, 346, 6211, 2014.
- 706 Romps, D. M.: Evaluating the future of lightning in cloud-resolving models. *Geophys. Res. Lett.*, 46. 2019.

707 Saha, U., Siingh, D., Kamra, A. K., Galanaki, E., Maitra, A., Singh, R. P., Singh, A. K., Chakraborty, S. and
708 Singh, R.: On the association of lightning activity and projected change in climate over the Indian sub-continent,
709 Atmos. Res., 183, 173-190, 2017.

710 Shi Z., Tana, Y. B., Tang H. Q, Sunc, J., Yanga, Y., Penga, L. and Guo, X.F.: Aerosol effect on land-ocean
711 contrast in thunderstorm electrification and lightning frequency, Atmos. Res., 164–165, 131–141, 2015.

712 Shi, Z., Tan, Y. B., Liu, Y., Liu, J., Lin, X., Wang, M. and Luan, J.: Effects of relative humidity on electrification
713 and lightning discharges in thunderstorms. Terr. Atmos. Ocean. Sci., 29, 695-708, [https://doi: 10.3319/
714 TAO.2018.09.06.01](https://doi.org/10.3319/TAO.2018.09.06.01), 2018

715 Shi Z, Wang H. C., Tan, Y. B., Li, L.Y. and Li, C. S.: Influence of aerosols on lightning activities in central
716 eastern China. Atmos Sci Lett., 21, e957. 2020.

717 Shindell, D. T., Faluvegi, G., Unger, N., Aguilar, E., Schmidt, G. A., Koch, D. M., Bauer, S. E. and Miller, R.
718 L.: Simulations of preindustrial, present-day, and 2100 conditions in the NASA GISS composition and climate
719 model G-PUCCINI. Atmos. Chem. Phys. 6, 4427–4459, 2006.

720 Singh, D., Singh, R. P., Singh, A. K., Kulkarni, M. N., Gautam, A. S. and Singh, A. K.: Solar activity, lightning
721 and climate. Surv. Geophys. 32, 659–703. 2011.

722 Takahashi, T.: Riming electrification as a charge separation mechanism in thunderstorms, J. Atmos. Sci., 35,
723 1536–1548, 1978.

724 Talukdar, S., Venkat Ratnam, M., Ravikiran, V. Chakraborty, R.: Influence of black carbon on atmospheric
725 instability. J. Geophys. Res.: Atmos., 124, 5539– 5554. 2019.

726 Taylor, K. E., Stouffer, R. J. and Meehl, G. A.: An Overview of CMIP5 and Experiment Design. Bull. Amer.
727 Meteor. Soc., 93, 485–498, 2012.

728 Twomey, S. A., Piepgrass, M. and Wolfe, T. L.: An assessment of the impact of pollution on global cloud
729 albedo. Tellus 36B, 356–366. 1984.

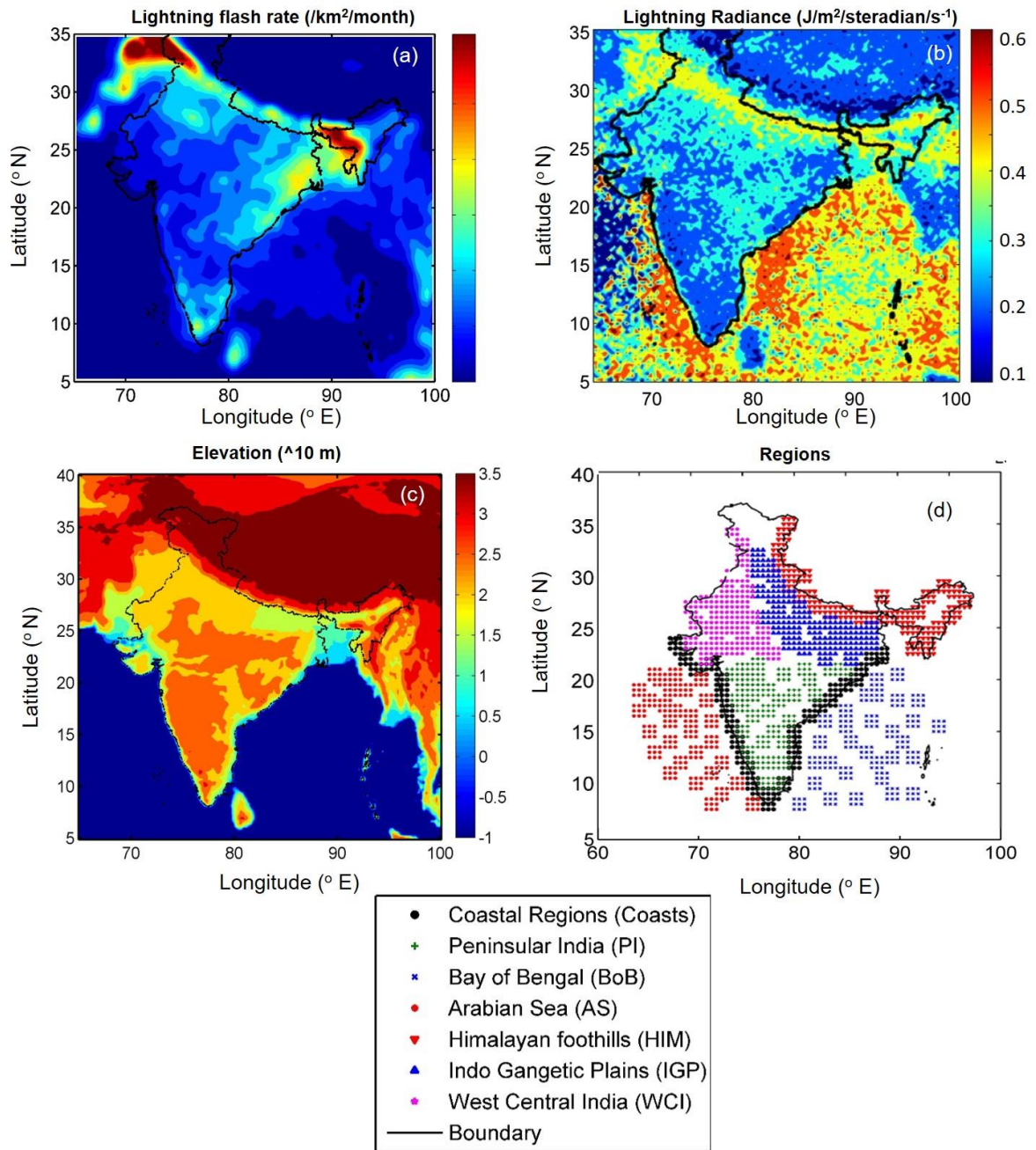
730 Uman, M.: All About Lightning Ch. 8, p. 68. Dover Publication Inc, 1986

731 van den Heever, S. C. and Cotton, W. R.: Urban aerosol impacts on downwind convective storms. J.
732 Appl. Meteorol. Climatol. 46, 828–850. 2007

733 Washington Post: [https://www.washingtonpost.com/world/lightning-strikes-kill-more-than-100-in-
734 india/2020/06/26/4c010886-b71c-11ea-9a1d-d3db1cbe07ce_story.html](https://www.washingtonpost.com/world/lightning-strikes-kill-more-than-100-in-india/2020/06/26/4c010886-b71c-11ea-9a1d-d3db1cbe07ce_story.html), last access: 19 September 2020

735 Williams, E. and Stanfill, S.: The physical origin of the land–ocean contrast in lightning activity. C. R. Phys. 3,
736 1277–1292, 2002.

737



738

739 **Figure 1:** Climatological mean (a) lightning flash rate, (b) lightning radiance over India averaged during 1998-2014. (c)
 740 Altitude above mean sea level in log10 scale (Seas denoted by -1) (d) Representation of seven regions used in the study

741

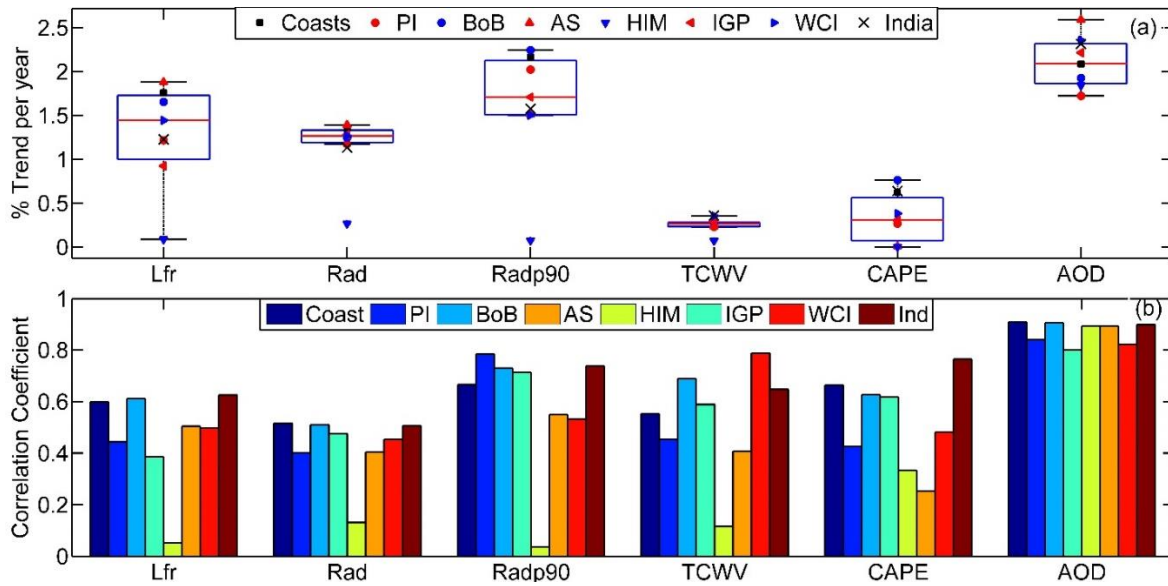
742

743

744

745

746



747

748 **Figure 2:** (a) % yearly trends in lightning flash rate (Lfr), Average radiance (Rad) and 90th percentile of radiance (Radp90)
 749 with TCWV, CAPE and AOD over seven regions and all India datasets. (b) Correlation coefficients corresponding to this trend
 750 values.

751

752

753

754

755

756

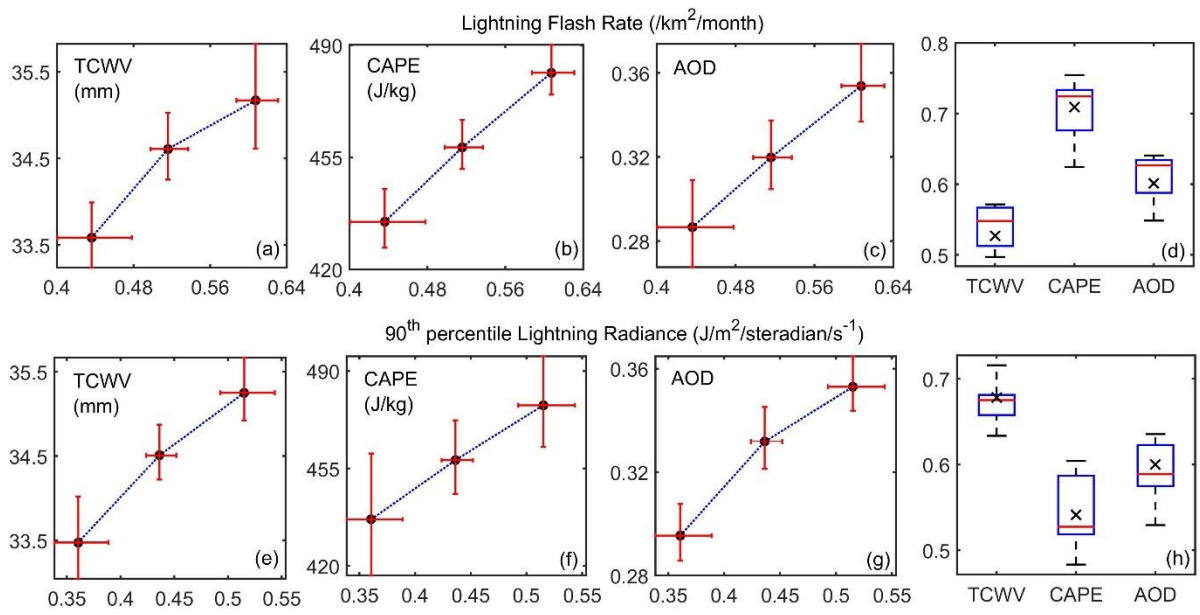
757

758

759

760

761



762

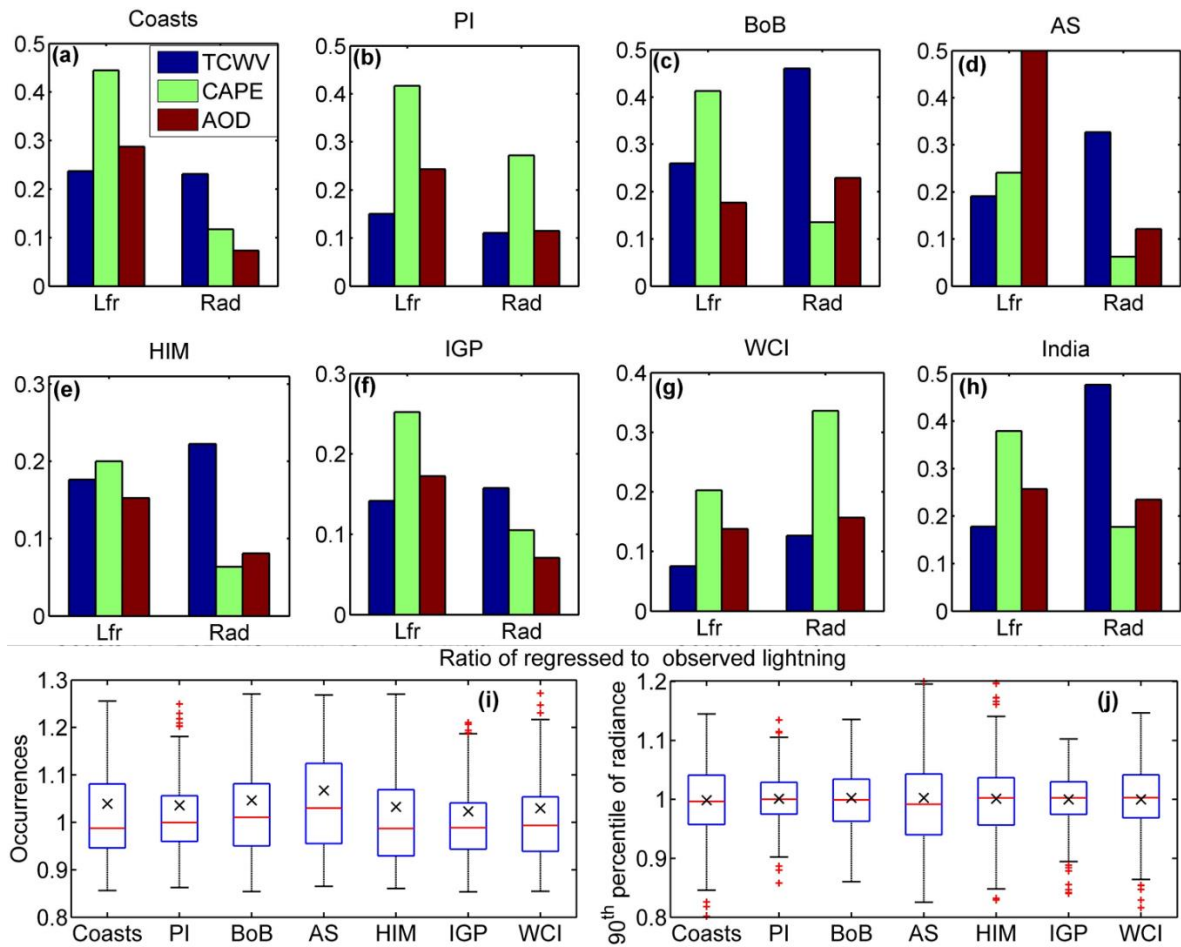
763 **Figure 3.** Temporal dominance cluster analysis results of lightning frequency and extreme radiances with respect to (a,e)
 764 TCWV, (b,f) CAPE and (c,g) AOD over entire Indian region, (d,h) distribution of correlation coefficient due to zonal clustering
 765 for both lightning parameters.

766

767

768

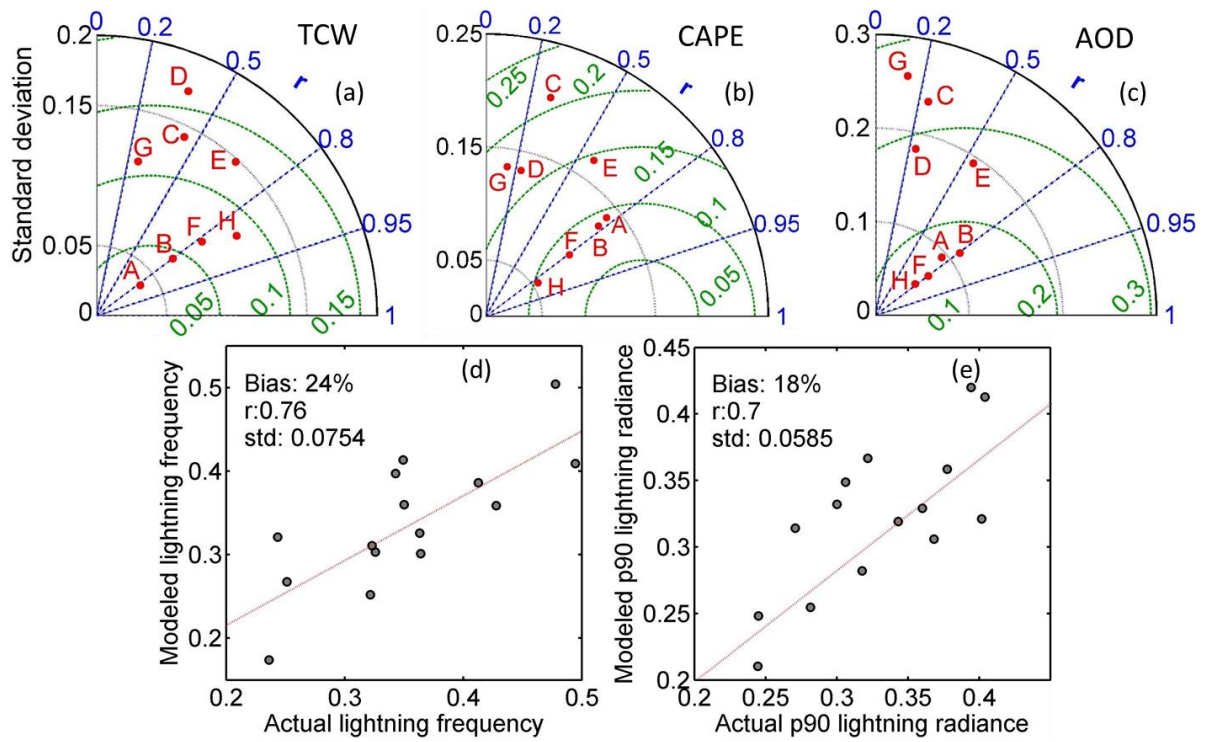
769



770

771 **Figure 4:** Temporal dominance analysis MLR coefficients of TCWV, CAPE and AOD for lightning frequency and radiance
 772 over (a) Coasts, (b) PI, (c) BoB, (d) AS, (e) HIM, (f) IGP, (g) WCI and (h) all India, (i,j) Zonal distribution of ratios between
 773 regressed and observed lightning frequency (Lfr) and 90th percentile of radiance (Radp90) over seven Indian regions.

774



775

776 **Figure 5:** Taylor diagram representing the performance of 8 GCMs used in the study with respect to (a) TCWV, (b) CAPE
 777 and (c) AOD, (d,e) Covariation between regressed lightning properties from model mean with respect to observations for
 778 average flash rate (/km²/month) and the 90th percentile of radiance (J/m²/steradian/s⁻¹).

779

780

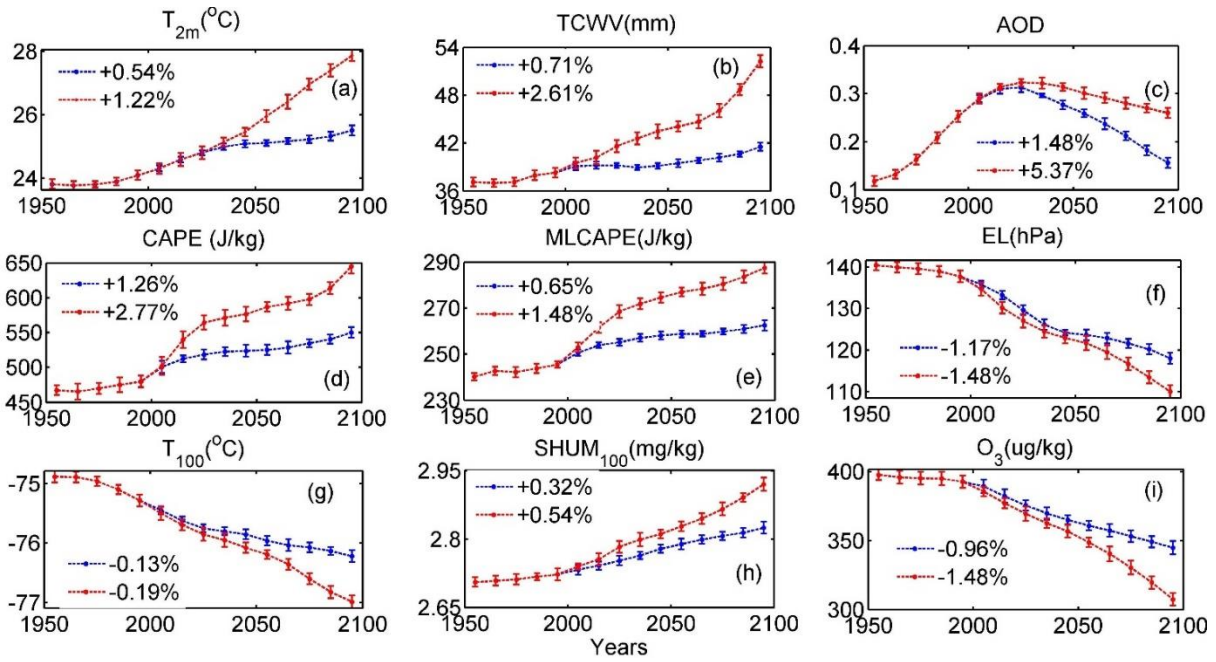
781

782

783

784

785



786

787 **Figure 6:** 150-year multi-model all-India average projections of various parameters using RCP 2.6 (blue) and RCP 8.5 (red)
 788 scenarios for (a) 2 metre temperature, (b) TCWV, (c) AOD, (d) CAPE, (e) MLCAPE, (f) EL, (g) Temperature 100 hPa, (h)
 789 Specific humidity, (i) Ozone mixing ratio same level. Legends indicate 5-yearly linear significant trends of these parameters.

790

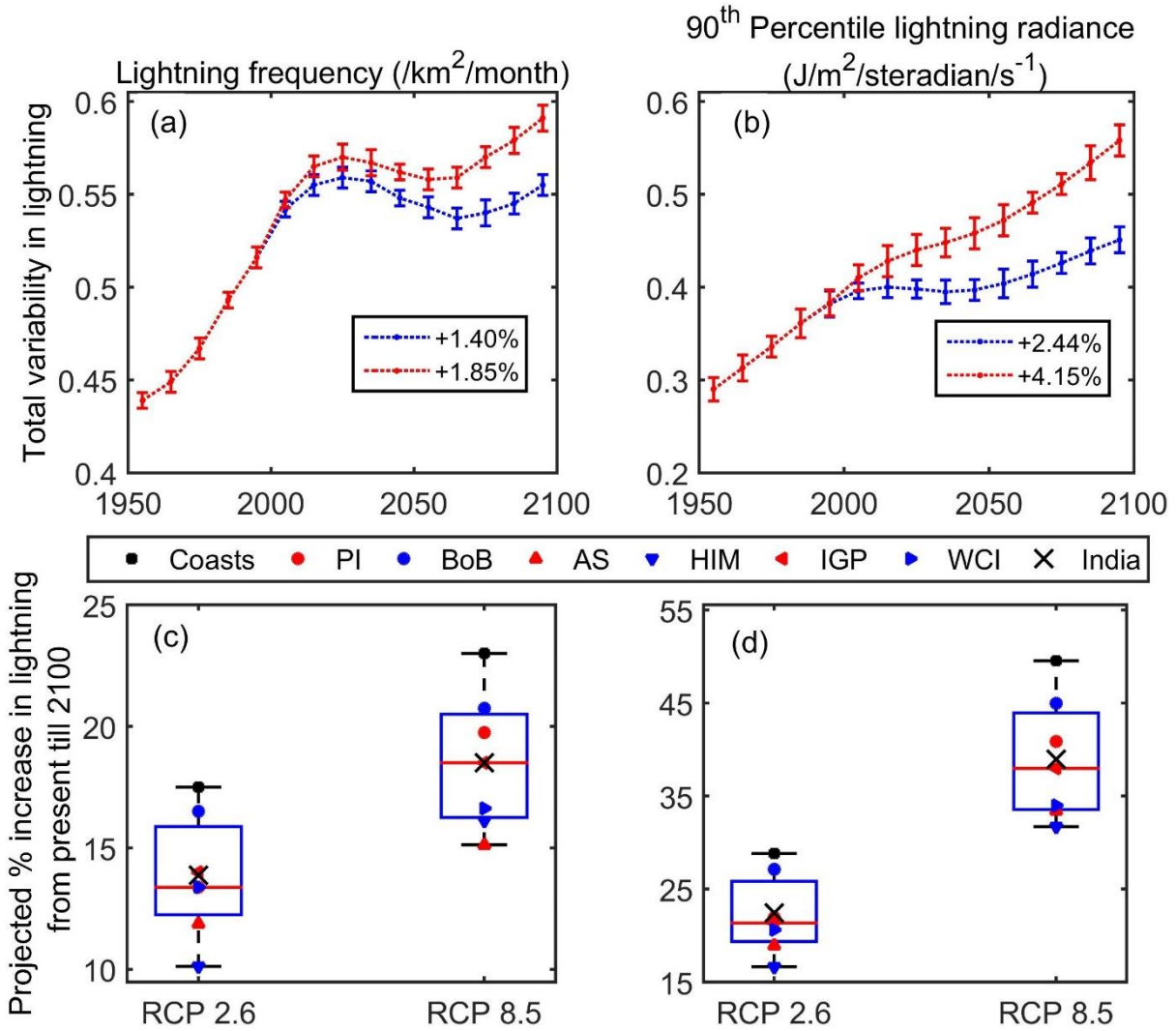
791

792

793

794

795



796

797 **Figure 7:** 150-year multi-model all-India average projections of (a) lightning occurrences and (b) 90th percentile radiance
798 using RCP 2.6 and RCP 8.5 scenarios (c,d) Zonal distribution of trends in lightning occurrence and intensity between present
799 decade (2011-2020) and 2091-2100. Legends in the top panel indicate the 5-yearly linear significant trends of these parameters.

800

801

802

803

804

805

806

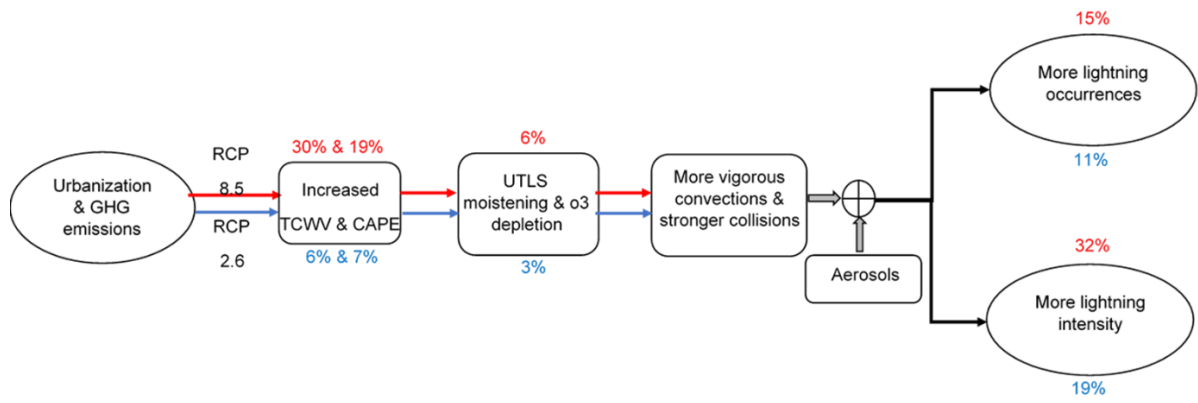
807

808

809

810

811



812

813

814

Figure 8: Proposed hypothesis to explain the long-term growth in lightning properties over Indian region between present (2016-2020) and the distant future (2096-2100) assuming RCP 2.6 and 8.5 scenarios shown in blue and red respectively.